

solve this inference problem. They range from analytical approximations [28] over stochastic approximations [29] to Bayesian inference using sophisticated particle methods [30, 31]. We point to Ref. [32] for an extensive list of references. There are also a number of contributions about theoretical properties of estimators in such systems [33]. However, there are some peculiarities about motility data that call for specialized methods.

The positional dynamics of active particles will often require a second order description. In macroscopic inertial systems like flocks of birds, second order dynamics arise naturally through the Newtonian equations of motion [6]. But also for microorganisms whose motion is usually governed by low Reynolds numbers and is therefore overdamped, a first order description might not be sufficient—if the complex propulsion mechanism generates a force with fluctuations that are best described by a first order Langevin equation, the positional dynamics become second order [12, 34]. This makes the observed positional process non-Markovian and does not allow for inference through transition density estimation.

Recently, new inference methods for homogeneous second order motility models have been introduced [35, 36]. However, these studies focus on the calculation of single point estimates for the motility parameters of each individual. In order to estimate the population heterogeneity from the available data in an optimal way, the full likelihood of the motility parameters is required. This is especially important if the measured trajectories have a short duration limiting the available information per trajectory. In the context of discrete time processes instead of continuous SDEs, motility inference based on likelihoods was discussed in Ref. [37]—the parameters inferred by this method will, however, depend on the sampling interval.

While individual trajectories may be very short, many experimental settings allow, however, for high sampling rates. This means that the relevant limit in this case is short measurement intervals τ while the total duration of the trajectories T remains constant. An inference method for motility data needs to be able to deal with potentially many data points per trajectory while converging to the true likelihood in the small τ limit.

In this work, we address the challenges summarized above by presenting a maximum likelihood based framework to infer distributions of motility parameters in heterogeneous ensembles of active particles. Maximum likelihood estimators (MLEs) are known to have favorable theoretical properties like consistency, equivariance and efficiency. To this end, we introduce a new way to approximate the likelihood of the parameters of the motility model with respect to single trajectories in second order settings. This method yields an analytical approximation to the likelihood with a concise functional form. The derivation has some parallels with the approach taken in Ref. [36]. In contrast to this previous work which considers a drift comprised of a linear velocity-dependent term and a non-linear position-dependent term, here, we

focus on models independent of position but with non-linear drift terms. We then plug this approximation into an expectation maximization (EM) scheme to obtain an MLE for the heterogeneity. Furthermore, we show how to obtain robust error estimates for the estimator. A methodologically different approximation of the likelihood in second order settings can be obtained using extended Kalman Filters [29, 38]. This provides a general approximation for partially observed systems by sequentially integrating out the unobserved parts of the system. This sequential algorithm, however, does not provide a closed-form expression for the likelihood and cannot provide intuitions about its parameter dependence.

The remainder of this paper is structured as follows. In Section II we introduce the model and details of the maximum likelihood approach. In Section III we demonstrate how naive approaches can fail for second order Langevin models and derive an approximate likelihood expression of the motility parameters. In Section IV we show how this approximation can be used to calculate a heterogeneity estimator together with its uncertainty. Finally, Section V presents the results of numerical experiments, before we end with some final remarks in Section VI.

II. MAXIMUM-LIKELIHOOD ESTIMATION FOR HETEROGENEOUS POPULATIONS

Let us consider the following model of a heterogeneous population of active particles, the velocity of which is modeled by some first order non-linear Langevin equation with additive noise. This leads to a second order model in the observed position:

$$\begin{cases} \dot{\mathbf{x}}^n(t) = & \text{motility} \\ \dot{\mathbf{v}}^n(t) = \mathbf{f}(\mathbf{v}^n(t); \boldsymbol{\eta}_f^n) + \sqrt{2D^n} \boldsymbol{\xi}^n(t) & \\ \boldsymbol{\eta}^n \sim p_{\boldsymbol{\eta}}(\cdot | \boldsymbol{\theta}^*) \text{ i.i.d.} & \text{heterogeneity} \\ \mathbf{x}_j^n = \mathbf{x}^n(t_0^n) + \int_{t_0^n}^{t_j^n} \mathbf{v}^n(t) dt & \text{observation.} \end{cases} \quad (1)$$

The Langevin equation depends on a number of parameters $\boldsymbol{\eta} \in \mathbb{R}^q$ which we call *motility parameters*. The motility parameters are split into a drift and a diffusion part $\boldsymbol{\eta}^n = \{\boldsymbol{\eta}_f^n, D^n\}$, \mathbf{f} is a smooth $\mathbb{R}^d \times \mathbb{R}^{q-1} \rightarrow \mathbb{R}^d$ function and $\boldsymbol{\xi}^n(t)$ are d -dimensional white noise processes with $\mathbb{E}[\boldsymbol{\xi}^n(t)(\boldsymbol{\xi}^m)^T(t')] = \mathbb{1} \delta_{nm} \delta(t-t')$. To account for heterogeneity within the population we assume that the motility parameters are a random variable which is independently drawn from a *heterogeneity distribution* $p_{\boldsymbol{\eta}}$ for each individual particle. Finally, this distribution is parametrized by parameters $\boldsymbol{\theta} \in \mathbb{R}^r$ which we call *heterogeneity parameters*. We denote the true heterogeneity parameters $\boldsymbol{\theta}^*$.

In an experiment, the positions of N particles are observed at fixed time intervals τ so that we measure a trajectory $\mathbf{T}^n = \{\mathbf{x}_j^n\}_{j=0,1,\dots,M^n}$ for each particle n , where the j^{th} position is recorded at time $t_j^n = t_0^n + j\tau$. The number of measurement points in trajectory n is

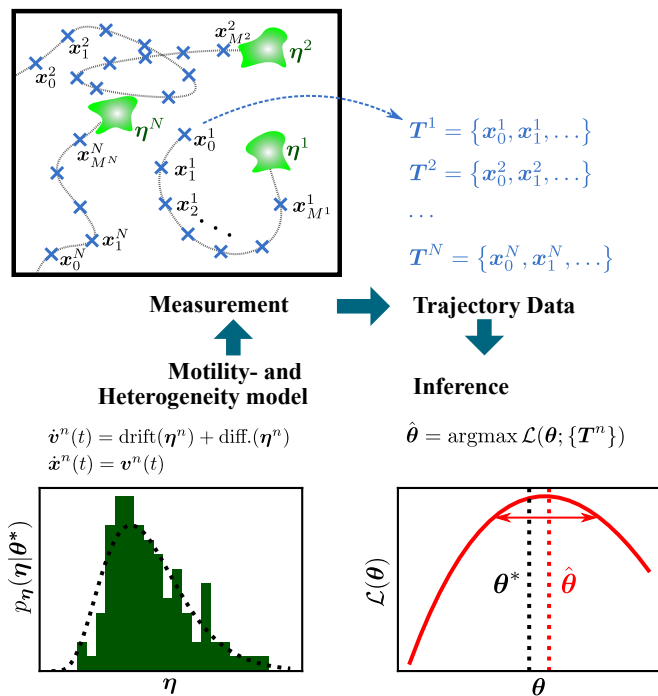


FIG. 1. Schematic sketch of heterogeneity inference. A stochastic motility model in velocity is assumed as well as a distribution p_η of the motility parameters η . This heterogeneity distribution has some true parameter θ^* . Each observed active particle moves with a given set of motility parameters η^n . Discretely sampled trajectories \mathbf{T}^n of the particles are measured. The likelihood of the heterogeneity parameters with respect to all measured trajectories is used to obtain an estimate $\hat{\theta}$. The curvature of the likelihood is a measure of uncertainty for the estimate.

then $M^n + 1$, so that M^n is the number of measured displacements. The duration of a trajectory is $T^n := t_{M^n}^n - t_0^n = M^n \tau$.

To characterize the system, we want to infer the heterogeneity within the population of particles from the observed discrete trajectories. Therefore, our main goal is to obtain an accurate estimate of the true heterogeneity parameters θ^* . Here, we will propose an approximate maximum likelihood estimator with respect to the whole set of trajectories $\{\mathbf{T}^n\}$. The log-likelihood $\mathcal{L}(\theta) := \log p(\{\mathbf{T}^n\} | \theta)$ is obtained by computing the joint probability of $\{\mathbf{T}^n\}$ and $\{\eta^n\}$ conditioned on θ and subsequently integrating out the unobserved motility parameters $\{\eta^n\}$:

$$\begin{aligned} \mathcal{L}(\theta) &= \sum_n \log p(\mathbf{T}^n | \theta) \\ &= \sum_n \log \int d\eta^n p(\mathbf{T}^n | \eta^n) p_\eta(\eta^n | \theta). \end{aligned} \quad (2)$$

The value $\hat{\theta}$ that maximizes this function is the maximum likelihood estimator (MLE) of θ . This estimator is expected to be asymptotically efficient.

An alternative estimation technique would be to calculate a single point estimate $\hat{\eta}^n$ for the motility parameter of each of the trajectories separately and then use this set of estimators $\{\hat{\eta}^n\}$ to estimate the heterogeneity [39, 40]. Such a two step approach avoids calculating the integrals in Eq. (2) but is oblivious to the uncertainty of each of these estimates $\hat{\eta}^n$. This leads to suboptimal inference especially in experimental settings where there is little data per trajectory and, thus, high uncertainty about the motility parameters. In contrast, the likelihood approach presented here encodes the uncertainty about each η^n in the term $p(\mathbf{T}^n | \eta^n)$, i. e. the likelihood of the motility parameter with respect to the individual measured trajectories. The integral then weights these uncertainties appropriately to obtain the likelihood of the heterogeneity parameters. Furthermore, this full likelihood approach enables an uncertainty estimate of $\hat{\theta}$ by analyzing the curvature of $\mathcal{L}(\theta)$ around its maximum,

$$H_{\alpha\beta} = \left. \frac{\partial}{\partial \theta^\alpha} \frac{\partial}{\partial \theta^\beta} \mathcal{L}(\theta) \right|_{\theta=\hat{\theta}}, \quad (3)$$

where upper Greek indices denote components of vectors.

The whole process from model over measurement to inference is shown schematically in Fig. 1.

Calculating the likelihood in Eq. (2) has two major challenges that need to be addressed. First, an approximation to the usually intractable log-likelihood for the motility parameters $\log p(\mathbf{T}^n | \eta)$ needs to be found. We call these likelihoods *single trajectory log-likelihoods*. While $p_\eta(\cdot | \theta)$ is given, the single trajectory likelihood $p(\mathbf{T} | \eta)$ needs to be derived from the motility model [cf. Eq. (1)]. The second order nature of the model requires to go beyond transition density estimates which are often employed for first order SDEs. Second, the integrals in Eq. (2) need to be addressed in order to maximize $\mathcal{L}(\theta)$. We will propose solutions to these challenges in the following two sections.

III. SINGLE TRAJECTORY LIKELIHOOD APPROXIMATION

A. Linear process as an illustrating example

For SDEs of first order, there are plenty of methods which provide parameter estimators as well as approximated likelihood expressions [41]. In this paper, we consider cases where only the integral of a first order process in velocity is observed which leads to a second order model in position. The instantaneous velocity process can be approximated from positional data by using finite differencing

$$\mathbf{V}_j = \frac{1}{\tau} \int_{t_j}^{t_{j+1}} dt \mathbf{v}(t) = \frac{\mathbf{x}_{j+1} - \mathbf{x}_j}{\tau}. \quad (4)$$

Following Ref. [12], we will refer to terms like \mathbf{V}_j as *secant velocities* in contrast to the instantaneous velocities $\mathbf{v}_j := \mathbf{v}(t_j)$. In the fast sampling limit of $\tau \rightarrow 0$,

the above approximation becomes exact. However, using estimation techniques for the first order process and plugging in the discrete approximation will lead to biases that persist even in the limit of $\tau \rightarrow 0$.

We demonstrate how these biases arise for a particularly simple system in which the drift term is linear, i. e. the velocity dynamics is described by an Ornstein-Uhlenbeck (OU) process:

$$\dot{\mathbf{v}}(t) = -\gamma \mathbf{v}(t) + \sqrt{2D} \boldsymbol{\xi}(t). \quad (5)$$

The advantage of this model is that all relevant expressions have a known analytic form.

If the process in Eq. (5) could be observed directly at constant time intervals τ , an Euler-style approximation to the log-likelihood with respect to the observations $\{\mathbf{v}_j\}$ would take the form

$$L_{v,\text{Eul}}(\gamma, D) = -\sum_j \left[\frac{d}{2} \log(\tau D) + \frac{(\Delta \mathbf{v}_j + \gamma \mathbf{v}_j \tau)^2}{4D\tau} \right] + C, \quad (6)$$

where $\Delta \mathbf{v}_j := \mathbf{v}_{j+1} - \mathbf{v}_j$ and C is a constant. By differentiation, the following maximum likelihood estimators for the two motility parameters can be derived

$$\hat{\gamma}_{v,\text{Eul}} = -\frac{\frac{1}{M_v} \sum_j \mathbf{v}_j \Delta \mathbf{v}_j}{\tau \frac{1}{M_v} \sum_k \mathbf{v}_k^2} \quad (7a)$$

$$\hat{D}_{v,\text{Eul}} = \frac{1}{2d\tau} \frac{1}{M_v} \sum_j (\Delta \mathbf{v}_j + \gamma \mathbf{v}_j \tau)^2, \quad (7b)$$

in which M_v is the number of terms in each of the sums. These estimators will be consistent in the limit of $\tau \rightarrow 0$. Since the instantaneous velocities cannot be observed, a naive approach would be to plug the finite difference approximation from Eq. (4) into the estimators derived from Eq. (6). This leads to the following estimators:

$$\hat{\gamma}_{\text{Eul}} = -\frac{\frac{1}{M_v} \sum_j \mathbf{V}_j \Delta \mathbf{V}_j}{\tau \frac{1}{M_v} \sum_k \mathbf{V}_k^2} \quad (8a)$$

$$\hat{D}_{\text{Eul}} = \frac{1}{2d\tau} \frac{1}{M_v} \sum_j (\Delta \mathbf{V}_j + \gamma \mathbf{V}_j \tau)^2. \quad (8b)$$

The OU process is ergodic. Therefore, we can replace the sums over j by expectation values in the limit of large M_v such that we obtain

$$\hat{\gamma}_{\text{Eul}} \approx -\frac{\mathbb{E}[\mathbf{V}_j \mathbf{V}_{j+1}] - \mathbb{E}[\mathbf{V}_j \mathbf{V}_j]}{\tau \mathbb{E}[\mathbf{V}_j^2]} \quad (9a)$$

$$\hat{D}_{\text{Eul}} \approx \frac{1}{2d\tau} \mathbb{E}[(\Delta \mathbf{V}_j + \gamma \mathbf{V}_j \tau)^2], \quad (9b)$$

Plugging in the true expressions for the covariances of \mathbf{V}_j (see Appendix A, Eqs. (A2b) and (A2c)) and taking the limit $\tau \rightarrow 0$, we obtain

$$\hat{\gamma}_{\text{Eul}} \rightarrow \frac{2}{3}\gamma, \quad \hat{D}_{\text{Eul}} \rightarrow \frac{2}{3}D. \quad (10)$$

This means that the ML estimate is biased even in the limit of high frequency sampling and long trajectories. The bias factor of 2/3 is typical for inference from integrals of processes driven by Brownian motion [42–45].

B. General failure of naive inference schemes for second order SDEs

In the previous section, we have shown the failure of naive inference schemes for the case of an OU process. We now take a step back and show why naive approaches fail on an abstract level.

In the previous section, we demonstrated that maximum likelihood estimators include expectation terms of the form $\mathbb{E}[\Delta \mathbf{V} \Delta \mathbf{V}]$ and $\mathbb{E}[h(\mathbf{V}) \Delta \mathbf{V}]$ in the limit of long trajectories. Terms like this depend on correlation structures on a time scale of τ . On long timescales, the statistics of the instantaneous and secant velocity become equivalent, since \mathbf{V} converges to \mathbf{v} . However, on small timescales comparable to τ , the statistics and correlation structure of \mathbf{v} and \mathbf{V} differ. This difference implies that the above expectations of the secant velocities do not converge to the corresponding expectations of the instantaneous velocities.

We consider the one-dimensional case for simplicity. In the stationary case, the following relation holds:

$$\begin{aligned} \mathbb{E}[\Delta V \Delta V] &= 2\{\mathbb{E}[V(0)V(0)] - \mathbb{E}[V(0)V(\tau)]\} \\ &= -2\mathbb{E}[V \Delta V]. \end{aligned} \quad (11)$$

With the definition of the secant velocity in Eq. (4), the two terms can be expressed as

$$\mathbb{E}[V(0)V(0)] = \frac{1}{\tau^2} \int_0^\tau dt' \int_0^\tau dt'' \mathbb{E}[v(t')v(t'')] \quad (12a)$$

$$\mathbb{E}[V(0)V(\tau)] = \frac{1}{\tau^2} \int_0^\tau dt' \int_\tau^{2\tau} dt'' \mathbb{E}[v(t')v(t'')]. \quad (12b)$$

If the velocity dynamics is a stationary diffusion process, the autocorrelation function is well approximated by $\mathbb{E}[v(0)v(t)] = c_0 + c_1|t| + \dots$ in a small region around zero with $c_0 = \mathbb{E}[v^2]$ and $c_1 = \mathbb{E}[v f(v)]$ (see Appendix B). Importantly, the coefficient c_1 is not zero, $c_1 \neq 0$, implying that the autocorrelation function is discontinuous at the origin. Using the above expansion, we find

$$\mathbb{E}[V(0)V(0)] = c_0 + \frac{1}{3}c_1\tau + \mathcal{O}(\tau^2), \quad (13a)$$

$$\mathbb{E}[V(0)V(\tau)] = c_0 + c_1\tau + \mathcal{O}(\tau^2). \quad (13b)$$

Plugging these results into Eq. (11), we eventually obtain

$$\mathbb{E}[\Delta V \Delta V] = -\frac{4}{3}c_1\tau = \mathbb{E}[\Delta v \Delta v] \left(\frac{2}{3} + \mathcal{O}(\tau) \right). \quad (14)$$

We find a similar equation for $\mathbb{E}[V \Delta V]$ and the result can be generalized to $\mathbb{E}[h(V) \Delta V]$. The bias factor of 2/3 here is the same factor that also appeared in Section III A.

Note, that this result is connected to the discontinuity of the velocity autocorrelation function at zero. It is well known for Gaussian processes that the behavior of the autocorrelation at zero is linked to the roughness of the process [46]. Therefore the bias arises due to the roughness of the underlying velocity process, which is driven by Gaussian white noise.

C. Likelihood approximation for non-linear drift functions

For diffusion processes with non-linear drift, there is no general analytic expression for the likelihood. Here, we derive an approximate expression for the likelihood with respect to positional observations when the motility model is of the form as in Eq. (1):

$$\dot{\mathbf{v}}(t) = \mathbf{f}(\mathbf{v}(t); \boldsymbol{\eta}_f) + \sqrt{2D} \boldsymbol{\xi}(t). \quad (15)$$

We expect the approximation to become accurate in the limit of rapid sampling $\tau \rightarrow 0$.

The general idea is to integrate both sides of the motility SDE to obtain an SDE in terms of secant velocities. This integrated SDE is driven by a colored noise term. Discretization together with a Gaussian approximation of the noise term then leads to the approximate likelihood expression. In the following derivations we will omit the $\boldsymbol{\eta}_f$ dependence of the drift \mathbf{f} for better readability. As before, we consider a single trajectory $\mathbf{T} = \{\mathbf{x}_j\}_{j=0, \dots, M}$ where the position of a particle is measured after constant time intervals τ .

First, we generalize the notion of *secant velocity* to arbitrary points in time:

$$\mathbf{V}^{(\tau)}(t) := \frac{1}{\tau} \int_t^{t+\tau} dt' \mathbf{v}(t') = \frac{\mathbf{x}(t+\tau) - \mathbf{x}(t)}{\tau}. \quad (16)$$

Formally, this time-continuous function $\mathbf{V}^{(\tau)}(t)$ is an integral transform of the instantaneous velocity $\mathbf{v}(t)$ and can also be viewed as a smoothing with a box kernel of width τ and height $1/\tau$. We use the superscript (τ) to stress that the definition of the time-continuous secant velocity depends on the measurement interval τ . Note that for $t = t_j$ with $j = 0, 1, \dots, M-1$, the value of the secant velocity can be obtained from the measured data as used in the previous sections.

We apply the integral transform in Eq. (16) to both sides of Eq. (15) and obtain an SDE for the secant velocity

$$\dot{\mathbf{V}}^{(\tau)}(t) = \mathbf{f}(\mathbf{V}^{(\tau)}(t)) + \sqrt{2D} \boldsymbol{\zeta}(t) + \mathcal{O}(\tau); \quad (17)$$

details on the transformation can be found in Appendix C. Note that this SDE has the same form as Eq. (15), but is driven by colored noise $\boldsymbol{\zeta}_t := \frac{1}{\tau} \int_t^{t+\tau} dt' \boldsymbol{\xi}(t')$ with a finite correlation time (cf. Appendix D) instead of white noise. From now on, we will omit the superscript (τ) for better readability.

Using the dynamics of $\mathbf{V}(t)$, we want to derive an expression for the joint probability of the measured secant velocities $\{\mathbf{V}(t_j) | j \in \{0, 1, \dots, M-1\}\}$. To this end, we integrate Eq. (17) over intervals $[t_j, t_{j+1}]$ and obtain

$$\mathbf{V}_{j+1} - \mathbf{V}_j - \int_{t_j}^{t_{j+1}} dt \mathbf{f}(\mathbf{V}(t)) = \sqrt{2D} \boldsymbol{\chi}_j + \mathcal{O}(\tau^2), \quad (18)$$

where $\boldsymbol{\chi}_j = \int_{t_j}^{t_{j+1}} dt \boldsymbol{\zeta}(t)$ is the integrated noise term and we abbreviated $\mathbf{V}(t_j) =: \mathbf{V}_j$. For each component α , the noise terms $\{\chi_j^\alpha\}$ are jointly normal distributed with zero mean and variance

$$\mathbf{Z} = \frac{\tau}{6} \begin{pmatrix} 4 & 1 & & & \\ 1 & 4 & 1 & & \\ & 1 & 4 & 1 & \\ & & & \ddots & \ddots & \ddots \end{pmatrix}; \quad (19)$$

see Appendix D for detailed calculations. The tridiagonal structure of \mathbf{Z} encodes the additional correlations in \mathbf{V}_j that are absent for \mathbf{v}_j .

We approximate the integral over the drift term using the trapezoidal rule:

$$\int_{t_j}^{t_{j+1}} dt f^\alpha(\mathbf{V}(t)) = \frac{\tau}{2} [f^\alpha(\mathbf{V}_j) + f^\alpha(\mathbf{V}_{j+1})] + R^\alpha(t). \quad (20)$$

The correction terms are summarized in R^α which scales like $\mathcal{O}(\tau^{3/2})$ in the small τ limit. With this, we obtain

$$\mathbf{V}_{j+1} - \mathbf{V}_j - \tau \bar{\mathbf{f}}(\mathbf{V}_j) = \sqrt{2D} \boldsymbol{\chi}_j + \mathcal{O}(\tau^{3/2}), \quad (21)$$

where we have used the short-hand $\bar{\mathbf{f}}(\mathbf{V}_j) := \frac{1}{2}[\mathbf{f}(\mathbf{V}_j) + \mathbf{f}(\mathbf{V}_{j+1})]$. In deterministic settings, the trapezoidal rule decreases the scaling of the correction terms with respect to simple Riemann-sum approximations. This is not the case in stochastic settings. However, using the trapezoidal rule removes $\mathcal{O}(\tau^2)$ contributions to the variance and covariance of the RHS of Eq. (21) which empirically improves the accuracy of the likelihood approximation.

We denote the LHS of Eq. (21)

$$\mathbf{Q}_j := \mathbf{V}_{j+1} - \mathbf{V}_j - \tau \bar{\mathbf{f}}(\mathbf{V}_j). \quad (22)$$

Since $\boldsymbol{\chi}_j$ is the leading order term of the RHS of Eq. (21), we approximate the probability of $\mathbf{Q}_{0:M-2}$ by the Gaussian probability of $\sqrt{2D} \boldsymbol{\chi}_{0:M-2}$. Thus, we have

$$p(\mathbf{Q}_{0:M-2}) \approx \prod_{\alpha} e^{-\frac{1}{4D} Q_i^\alpha [\mathbf{Z}^{-1}]_{ij} Q_j^\alpha} \det(4\pi D \mathbf{Z})^{-1/2}, \quad (23)$$

where we use Einstein's summation convention for indices i and j .

In order to obtain the likelihood of the parameters with respect to the secant velocities, we convert the probability of $\mathbf{Q}_{0:M-2}$ into a probability of $\mathbf{V}_{1:M-1}|\mathbf{V}_0$ by multiplying the appropriate Jacobi determinant of the transformation. Because \mathbf{Q}_j only depends on \mathbf{V}_j and \mathbf{V}_{j+1} , the determinant factorizes and we obtain (see Appendix E)

$$\prod_{j=1}^{M-1} \left| \det \mathbf{J}[\mathbf{g}(z)]|_{z=\mathbf{V}_j} \right| \quad \text{with} \quad \mathbf{g}(z) := z - \frac{\tau}{2} \mathbf{f}(z), \quad (24)$$

where $\mathbf{J}[\cdot]$ denotes the Jacobi matrix. Further multiplication of the steady state distribution of \mathbf{V}_0 yields the probability of $\mathbf{V}_{0:M-1}$ which now includes the first measured secant velocity \mathbf{V}_0 . Because this steady state distribution, in general, does not have an analytic expression, we use the steady state distribution of the instantaneous velocity $p_{\mathbf{v}}$ as an approximation instead.

The above considerations lead to the following approximation for the probability of the measured secant velocities:

$$p(\mathbf{V}_{0:M-1}|\boldsymbol{\eta}) \approx p_{\mathbf{v}}(\mathbf{V}_0|\boldsymbol{\eta}) \prod_{\alpha} \left[\exp\left(-\frac{1}{4D} Q_i^{\alpha} [\mathbf{Z}^{-1}]_{ij} Q_j^{\alpha}\right) \det(4\pi D \mathbf{Z})^{-1/2} \right] \prod_{j=1}^{M-1} \left| \det \left(\mathbb{1} - \frac{\tau}{2} \mathbf{J}[\mathbf{f}(z)]|_{z=\mathbf{V}_j} \right) \right| \quad (25)$$

Remember that the drift function \mathbf{f} , and through it Q_i^{α} , depend on the motility parameters.

Taken as a function of the motility parameters $\boldsymbol{\eta}$, the expression in Eq. (25) is an approximation to the likelihood of the motility parameters with respect to the measured secant velocities, which we abbreviate $p_{\text{tG}}(\mathbf{V}_{0:M-1}|\boldsymbol{\eta})$ in the following. Because we assume the probability of the first measured position \mathbf{x}_0 to be uniform over the observation space, the likelihood in terms of the positions is identical to the likelihood in terms of the secant velocities up to a τ dependent constant:

$$L(\boldsymbol{\eta}) := \log p(\mathbf{T}|\boldsymbol{\eta}) = \log p(\mathbf{V}_{0:M-1}|\boldsymbol{\eta}) + C \\ \approx \log p_{\text{tG}}(\mathbf{V}_{0:M-1}|\boldsymbol{\eta}) + C. \quad (26)$$

The expression for the likelihood in Eq. (25) is a transformation of the multivariate Gaussian distribution of $\mathbf{Q}_{0:M-2}$; therefore we will call this approximation to the likelihood *transformed Gaussian* method. Note, however, that Eq. (25) is generally non-Gaussian with respect to the secant velocities due to the nonlinear drift \mathbf{f} .

Numerical evaluation of $p_{\text{tG}}(\mathbf{V}_{0:M-1}|\boldsymbol{\eta})$ requires the calculation of the Gaussian density of $\mathbf{Q}_{0:M-2}$ in square brackets. In Appendix F, we show that this can be done in $\mathcal{O}(M)$ steps without explicit inversion of \mathbf{Z} due to its tridiagonal structure.

To illustrate the validity and effectivity of the derived approximation to the single-particle likelihood $L(\boldsymbol{\eta})$, results of maximum likelihood inference of motility parameters on the basis of the transformed Gaussian approximation [Eq. (25)] are plotted in Fig. 2 for a paradigmatic motility model for active particles in two spatial dimensions [2, 47]:

$$\dot{\mathbf{x}} = \mathbf{v}, \quad (27a)$$

$$\dot{\mathbf{v}} = -\gamma \mathbf{v}(v^2 - v_r^2) + \omega \begin{pmatrix} 0 & -1 \\ 1 & 0 \end{pmatrix} \mathbf{v} + \sqrt{2D} \boldsymbol{\xi}(t). \quad (27b)$$

Here, $v = |\mathbf{v}|$ denotes the speed of the particle and the motility parameters are $\boldsymbol{\eta} = (\gamma, \omega, v_r, D)$. The drift term corresponds to a Mexican-hat potential with preferred speed v_r . Additionally there is a chiral term which makes the particles rotate. The plots show that the transformed Gaussian method for the approximation of the likelihood

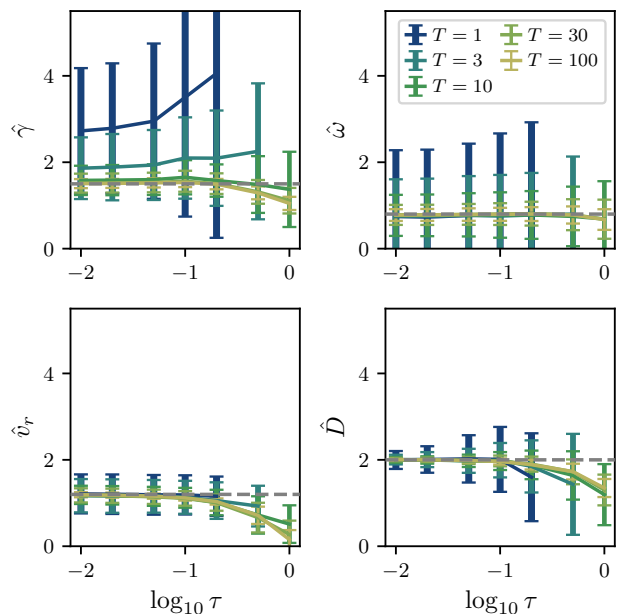


FIG. 2. Maximum likelihood estimates for motility parameters of model [Eq. (27)]. The estimates were obtained by numerical maximization of the transformed Gaussian approximation of the likelihood. The plots show mean and standard deviation of inferred parameters from 100 simulated trajectories. The input parameter values of the simulation are shown as gray dashed lines. For different values of T , the same set of trajectories was used and appropriately shortened.

leads to consistent estimates of the motility parameters for sufficiently small measurement intervals τ . Only for estimation of the γ parameter a minimum total recording time $T = M\tau$ of the trajectory is required to obtain consistent estimates. As γ is connected to the persistence time of the trajectories, short trajectories contain little information about this parameter. As expected, the spread of the estimates for each of the parameters decreases with increasing trajectory length as the additional information allows for more accurate inference.

IV. LIKELIHOOD MAXIMIZATION

In the previous part, we have introduced an approximation to the single-particle likelihoods $L_n(\boldsymbol{\eta})$ of the motility parameters. These likelihoods enter in the expression for the likelihood $\mathcal{L}(\boldsymbol{\theta})$ of the heterogeneity parameters [Eq. (2)]. In this section, we will show how that approximation can be used to maximize $\mathcal{L}(\boldsymbol{\theta})$ and find an MLE for the heterogeneity parameters $\boldsymbol{\theta}$.

A. Maximum Likelihood Estimation via stochastic EM algorithm

The expression for the log-likelihood of the heterogeneity parameters in Eq. (2) contains integrals over the motility parameters. In general, there is no analytic solution for these integrals. Instead of evaluating them numerically [28], we propose here to use an expectation-maximization (EM) algorithm [48] in a similar way as in Ref. [29]. The EM algorithm is commonly used in systems with latent variables because it provides a structured way to approach a local maximum of the likelihood in such situations. Furthermore, it does not depend on a certain functional form and, thus, we are free in the choice of a heterogeneity model. In our case, the latent variables are the unobserved true motility parameters $\{\boldsymbol{\eta}^n\}$ of the individual trajectories. The algorithm avoids evaluation of the integrals over the unobserved variables and instead relies on calculation of expectation values, which can be approximated through sampling.

The EM algorithm is initialized by some initial guess for the heterogeneity parameters $\hat{\boldsymbol{\theta}}_0$. It then iteratively creates a sequence of estimates $\{\hat{\boldsymbol{\theta}}_i\}$ such that the sequence of corresponding log-likelihood values $\{\mathcal{L}(\hat{\boldsymbol{\theta}}_i)\}$ is monotonously increasing: if $j > i$, then $\mathcal{L}(\hat{\boldsymbol{\theta}}_j) \geq \mathcal{L}(\hat{\boldsymbol{\theta}}_i)$. This is achieved by the following iteration rule: the next $\hat{\boldsymbol{\theta}}_{i+1}$ is given by

$$\hat{\boldsymbol{\theta}}_{i+1} = \underset{\boldsymbol{\theta}}{\operatorname{argmax}} \sum_n \int d\boldsymbol{\eta} p(\boldsymbol{\eta}|\mathbf{T}^n, \hat{\boldsymbol{\theta}}_i) \log p(\mathbf{T}^n, \boldsymbol{\eta}|\boldsymbol{\theta}) \quad (28a)$$

$$= \underset{\boldsymbol{\theta}}{\operatorname{argmax}} \sum_n \mathbb{E}_{n,i}[\log p_{\boldsymbol{\eta}}(\boldsymbol{\eta}|\boldsymbol{\theta})], \quad (28b)$$

where $\mathbb{E}_{n,i}[\cdot]$ denotes an expectation value with respect to the conditional probability distribution for the motility

parameters $p(\boldsymbol{\eta}|\mathbf{T}^n, \hat{\boldsymbol{\theta}}_i)$. In deriving Eq. (28b), we used that

$$\log p(\mathbf{T}^n, \boldsymbol{\eta}|\boldsymbol{\theta}) = \log p(\mathbf{T}^n|\boldsymbol{\eta}) + \log p_{\boldsymbol{\eta}}(\boldsymbol{\eta}|\boldsymbol{\theta}), \quad (29)$$

where the first term on the RHS does not depend on $\boldsymbol{\theta}$. The algorithm stops when a certain stop criterion is met. Here, we end the iteration once the change in each component of $\hat{\boldsymbol{\theta}}_i$ falls below a small value ε .

Since the conditional distribution of the motility parameters is proportional to the joint distribution

$$p(\boldsymbol{\eta}|\mathbf{T}^n, \hat{\boldsymbol{\theta}}_i) \sim p(\mathbf{T}^n, \boldsymbol{\eta}|\hat{\boldsymbol{\theta}}_i) = p(\mathbf{T}^n|\boldsymbol{\eta}) p_{\boldsymbol{\eta}}(\boldsymbol{\eta}|\hat{\boldsymbol{\theta}}_i), \quad (30)$$

we can draw samples from $p(\boldsymbol{\eta}|\mathbf{T}^n, \hat{\boldsymbol{\theta}}_i)$ using the known heterogeneity model and the approximated likelihood of the motility parameters from the previous section [Eq. (25)]. With these samples, we can approximate the expectation values using sample averages.

The procedure described above is, however, computationally expensive since we have to resample at each iteration step for each of the measured trajectories. In order to accelerate the calculations, we employ so called importance sampling [49, chap. 3.3]. The main idea is that samples drawn from some distribution can be used to estimate averages with respect to another distribution by an appropriate weighting. In our case the sampling distribution naturally decomposes into the likelihood $p(\mathbf{T}^n|\boldsymbol{\eta})$ and the heterogeneity distribution $p_{\boldsymbol{\eta}}(\boldsymbol{\eta}|\hat{\boldsymbol{\theta}}_i)$, where only the latter depends on the current estimate $\hat{\boldsymbol{\theta}}_i$. We can therefore create samples proportionally to each single trajectory likelihood $\exp L_n(\boldsymbol{\eta}) := p(\mathbf{T}^n|\boldsymbol{\eta})$ once using the transformed Gaussian approximation [Eq. (25)]. These samples can then be reused in each step of the EM algorithm with appropriate weighting factors:

$$\mathbb{E}_{n,i}[h(\boldsymbol{\eta})] \approx \frac{1}{L} \sum_{l=1}^L p_{\boldsymbol{\eta}}(\check{\boldsymbol{\eta}}_l|\hat{\boldsymbol{\theta}}_i) h(\check{\boldsymbol{\eta}}_l), \quad (31)$$

with $\check{\boldsymbol{\eta}}_l \sim \exp L_n(\boldsymbol{\eta})$ and where $h(\cdot)$ is an arbitrary function of the motility parameters. Care needs to be taken, because $p(\mathbf{T}^n|\boldsymbol{\eta})$ is not necessarily normalizable when taken as a function of $\boldsymbol{\eta}$. By restricting the sampling space to some finite volume of the parameter space or multiplying a decaying function that ensures normalizability, we can still use the likelihood as a basis for sampling.

B. Uncertainty estimate via Hessian Matrix

The EM algorithm yields an approximate maximum likelihood estimator $\hat{\boldsymbol{\theta}}$ for the heterogeneity parameters. In order to judge the reliability of this estimate, we want to estimate the uncertainty of $\hat{\boldsymbol{\theta}}$. This can be done by calculating the Hessian matrix \mathbf{H} , i. e. the second deriva-

tive, of the log-likelihood $\mathcal{L}(\boldsymbol{\theta})$ at $\hat{\boldsymbol{\theta}}$:

$$H_{\alpha\beta} = \frac{\partial}{\partial\theta_\alpha} \frac{\partial}{\partial\theta_\beta} \sum_n \log p(\mathbf{T}^n|\boldsymbol{\theta}) \Big|_{\boldsymbol{\theta}=\hat{\boldsymbol{\theta}}}. \quad (32)$$

First, if the likelihood is assumed to be a non-normalized Gaussian distribution, the negative inverse of the Hessian matrix corresponds to correlation matrix of this distribution. From a Bayesian perspective, the Hessian matrix therefore determines where the majority of the posterior mass is concentrated given a flat prior. Second, the negative Hessian matrix is an empirical estimate of the Fisher information $\mathcal{I}(\boldsymbol{\theta}^*)$ about the heterogeneity parameters contained in the given set of trajectories. Typically, the fluctuations of an MLE around the true value converge in distribution to a normal distribution [50, chap. 7.3]:

$$\sqrt{N}(\hat{\boldsymbol{\theta}} - \boldsymbol{\theta}^*) \xrightarrow{D} \mathcal{N}(0, \mathcal{I}^{-1}(\boldsymbol{\theta}^*)) \quad \text{as } N \rightarrow \infty, \quad (33)$$

This property is called asymptotic normality and implies that the stochastic fluctuations of the MLE $\hat{\boldsymbol{\theta}}$ are directly connected to the Fisher Information in the limit of many trajectories in the dataset. This means that we can use the negative inverse Hessian matrix \mathbf{H} to obtain an estimate of the standard deviation of $\hat{\boldsymbol{\theta}}$.

After a few manipulations (see Appendix G), we find that the elements of the Hessian matrix can be expressed as

$$H_{\alpha\beta} = \sum_n \left[\mathbb{E}_n \left[\frac{\partial_\alpha \partial_\beta p_\eta(\boldsymbol{\eta}|\boldsymbol{\theta})}{p_\eta(\boldsymbol{\eta}|\boldsymbol{\theta})} \right] - \mathbb{E}_n \left[\frac{\partial_\alpha p_\eta(\boldsymbol{\eta}|\boldsymbol{\theta})}{p_\eta(\boldsymbol{\eta}|\boldsymbol{\theta})} \right] \mathbb{E}_n \left[\frac{\partial_\beta p_\eta(\boldsymbol{\eta}|\boldsymbol{\theta})}{p_\eta(\boldsymbol{\eta}|\boldsymbol{\theta})} \right] \right] \Big|_{\boldsymbol{\theta}=\hat{\boldsymbol{\theta}}}, \quad (34)$$

where $\mathbb{E}_n[\cdot]$ denotes an expectation with respect to $p(\boldsymbol{\eta}|\mathbf{T}^n, \hat{\boldsymbol{\theta}})$ and we have used the abbreviation $\partial_\alpha := \partial/\partial\theta^\alpha$. This turns out to be a slightly modified version of Louis' formula [29, 51]. Conveniently, the expectations can be approximated analogous to Eq. (31) using the same set of samples that have been used in the EM algorithm.

V. RESULTS

A. Convergence

In the previous sections, we have described an inference scheme to estimate the heterogeneity parameters of a population of active particles from trajectory data. In this section, we demonstrate through numerical experiments that this approach can indeed recover an input heterogeneity.

In the setting that we are considering in this paper, the primary interest is finding the heterogeneity distribution $p_\eta(\boldsymbol{\eta}|\boldsymbol{\theta})$. In this sense the estimated heterogeneity

parameters $\hat{\boldsymbol{\theta}}$ are merely an aid for finding the shape of the distribution. To judge the performance of the inference scheme, we therefore choose to use the Kullback-Leibler (KL) divergence as a measure of similarity between distributions rather than the distance in parameter space.

We will compare the heterogeneity distribution inferred from the measured data, i. e. the trajectories, to the hypothetical case in which the hidden motility parameters $\{\boldsymbol{\eta}_n\}$ are known. Given $\{\boldsymbol{\eta}_n\}$, we use the maximum likelihood estimator $\hat{\boldsymbol{\theta}}_\eta := \text{argmax}_\boldsymbol{\theta} \sum_n \log p_\eta(\boldsymbol{\eta}^n|\boldsymbol{\theta})$ to estimate the heterogeneity parameters. We use this as the baseline rather than the true input distribution because the trajectories cannot contain more information about the true heterogeneity distribution than the information contained in the hidden, finite set of motility parameters. In this sense, $\boldsymbol{\theta}_\eta$ represents the best possible guess from the given number of trajectories.

In addition to inference by maximization of the full likelihood $\mathcal{L}(\boldsymbol{\theta})$, cf. Eq. (2), we also consider the alternative two stage approach that has already been touched upon in Section II. This approach first uses the transformed Gaussian approximation to obtain a single point MLE for the motility parameters $\hat{\boldsymbol{\eta}}^n$ of each trajectory. In a second step we then use only these estimates to obtain an MLE of the heterogeneity parameter $\hat{\boldsymbol{\theta}} := \text{argmax}_\boldsymbol{\theta} \sum_n \log p_\eta(\hat{\boldsymbol{\eta}}^n|\boldsymbol{\theta})$.

As an example, we consider the following two-dimensional system with motility model [2]

$$\dot{\mathbf{x}} = \mathbf{v} \quad (35a)$$

$$\dot{\mathbf{v}} = -\gamma \mathbf{v} (v^2 - v_r^2) + \sqrt{2D} \boldsymbol{\xi}(t) \quad (35b)$$

and heterogeneity model given by

$$p_\eta(\boldsymbol{\eta}|\boldsymbol{\theta}) = q_\Gamma(\gamma|\alpha_\gamma, \beta_\gamma) q_\Gamma(v_r|\alpha_{v_r}, \beta_{v_r}) q_\Gamma(D|\alpha_D, \beta_D), \quad (36)$$

in which

$$q_\Gamma(x|\alpha, \beta) = \frac{\beta^\alpha}{\Gamma(\alpha)} x^{\alpha-1} e^{-\beta x} \quad (37)$$

is the density of a Γ -distribution. The above motility model is a version of Eq. (27) with zero chirality ($\omega = 0$). The model has three motility parameters $\boldsymbol{\eta} = (\gamma, v_r, D)$ and a six dimensional heterogeneity parameter

$$\boldsymbol{\theta} = (\alpha_\gamma, \beta_\gamma, \alpha_{v_r}, \beta_{v_r}, \alpha_D, \beta_D). \quad (38)$$

The results for the inference of this model are shown in Fig. 3. Since the heterogeneity distribution for the three motility parameters factorizes in this model, the results for each motility parameter can be plotted individually.

For a fixed duration T of the trajectories, the inferred distributions are the closer to the baseline the shorter the sampling interval τ is. The information about the drift contained in a continuous trajectory is limited by

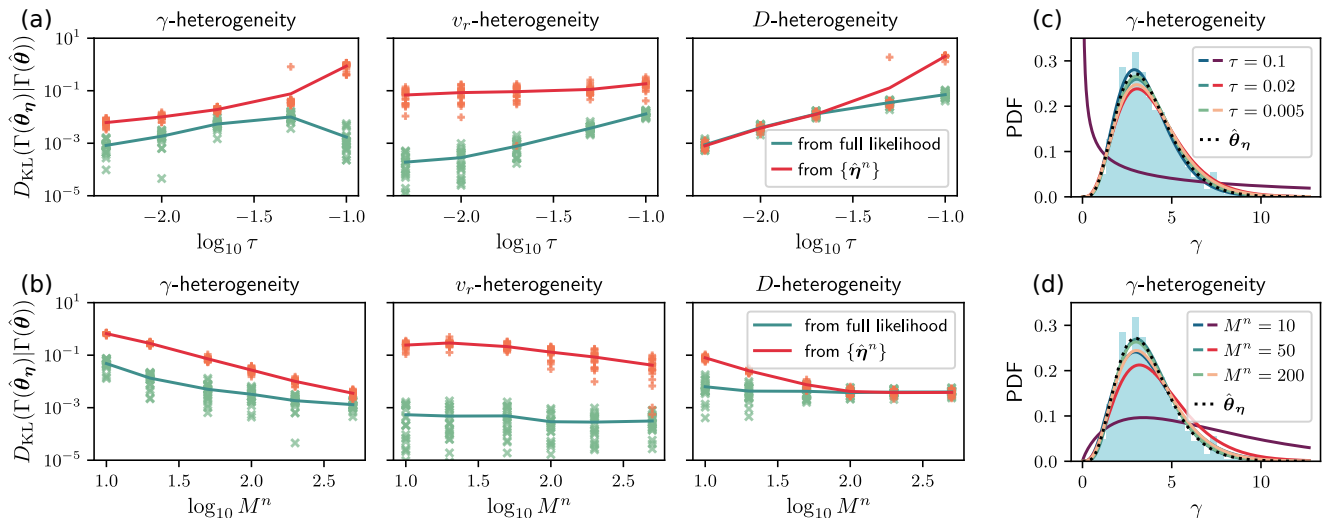


FIG. 3. KL-divergence between the heterogeneity distributions inferred using hidden motility parameters and inferred using the observed trajectories. The green curves show the estimate obtained using the full likelihood $\mathcal{L}(\theta)$. The red curves show the results for a two stage estimate where first the motility parameter is estimated for each trajectory and these estimates $\{\hat{\eta}^n\}$ are subsequently used to estimate the heterogeneity. The underlying motility and heterogeneity model are given in Eqs. (35, 36). In (a) the dependence on sampling interval τ for fixed $T^n = 2.0$ is shown; in (b) the dependence on number of sample points M^n with fixed $\tau = 0.01$. For each parameter combination, the results of 20 realizations of datasets with $N = 500$ trajectories are shown. The solid lines are averages. The input heterogeneity parameters are $\theta = (\alpha_\gamma, \beta_\gamma, \alpha_{v_r}, \beta_{v_r}, \alpha_D, \beta_D) = (5.5, 1.5, 5.5, 1.5, 5.5, 0.5)$. Panels (c) and (d) show the inferred probability density functions for individual realizations of a data set as a function of τ and M^n , respectively. For reference, the histogram shows the empirical distribution of the motility parameter which is kept the same for all choices for τ and M^n .

the duration of the trajectory—the improvement in the inference for the drift parameters is mostly due to the improved accuracy of the likelihood. When considering longer and longer trajectories with fixed sampling intervals on the other hand, the improved accuracy of the inference is due to the additional information contained in longer trajectories. The available information about the diffusion term, on the other hand, depends on the sampling interval. Therefore, the accuracy of the inferred distribution increases with decreasing τ , but is largely independent of the trajectory duration or number of measurement points in a trajectory.

Inference from the full likelihood implicitly takes into account all possible values for the motility parameters and weights them according to the single trajectory likelihood. If there is a lot of information, the single trajectory likelihood is sharp and the weighting function approaches a delta distribution. In this case the inferred heterogeneity from the full likelihood will be almost identical to the inference from the single point estimates. In our case, the single trajectory likelihood in D -direction becomes very sharp for many data points and/or short sampling intervals. In these limits, the inferred heterogeneity is the same for both methods. On the other hand, little information per trajectory leads to large deviations between the two approaches as can be seen for the drift parameters at short trajectory durations in Fig. 3.

B. Asymptotic normality

In Section IV B we have introduced the Hessian matrix as a way to estimate the uncertainty of the MLE $\hat{\theta}$. While it still remains to be proven that asymptotic normality of the MLE is fulfilled in our specific case [33], we can collect numerical evidence that the Hessian matrix provides a good uncertainty estimate in practice.

We again use the model from the previous section [Eqs. (35-38)] as an example. Figure 4 shows the inference results on $R = 100$ realizations of datasets from this model with identical heterogeneity parameters. Here, we use datasets comprised of $N = 200$ trajectories of duration $T^n = 0.5$. In contrast to the previous section, the results are shown in parameters space since asymptotic normality is a statement about the distribution in this space.

The mean of the inferred parameters $\hat{\theta}_R = (1/R) \sum_r \hat{\theta}_r$ is close to the true input parameters of the simulations as is expected from the results of the previous section. Furthermore, we observe that the standard deviation of the estimates closely matches the uncertainty estimate obtained from the averaged Hessian matrix $\bar{\mathbf{H}}(\hat{\theta}_R) = (1/R) \sum_r \mathbf{H}_r(\hat{\theta}_R)$ around $\hat{\theta}_R$. The largest deviation occurs for the parameter γ . It controls the relaxation time of the system and is most sensitive to the duration of the trajectory.

These numerical experiments demonstrate heuristi-

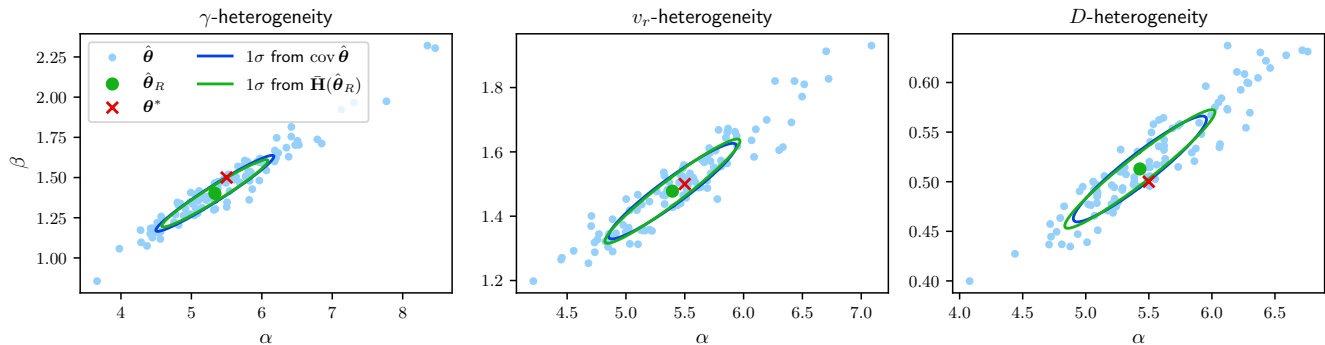


FIG. 4. Inferred heterogeneity parameters from $R = 100$ realizations of trajectory sets with identical heterogeneity parameters θ^* . The mean of the inferred parameters over all realizations is denoted by $\hat{\theta}_R$. The blue ellipses correspond to the covariance of the estimates while the green ellipses are calculated from the average Hessian matrix of the log-likelihood. Each dataset contains $N = 200$ trajectories with sampling interval $\tau = 0.01$ and length $M^n = 50$ which corresponds to a duration $T^n = 0.5$. The model and parameter values are the same as in Fig. 3.

cally that we can obtain information about the spread of the estimators from the shape of the likelihood and that the uncertainty estimate obtained via the Hessian matrix is indeed meaningful.

VI. CONCLUSION

We proposed a methodology to estimate the heterogeneity of a population of active particles from discrete trajectory data. We opted for a full likelihood approach as this utilizes the available data efficiently, allows for consistent uncertainty measures of the estimate, and outperforms alternative two level approaches especially in the limit of short trajectories. We show that the approach successfully separates the two sources of stochasticity in the data: the temporal fluctuations of the trajectories and the variability between the individuals. This way, it opens the door to quantitative modeling of heterogeneous motile particle ensembles.

At the heart of the method is a new approximation of the single trajectory likelihood for second order Langevin models. The second order nature of the model makes the observed processes non-Markovian, which requires more involved approximation techniques than in the case of first order models. Our approximation approach is in the spirit of the *first integrate then discretize* approach in Ref. [36]. We considered finite difference approximations to the instantaneous velocities, which we call secant velocities. These are effectively driven by colored noise, so they have different correlations from the instantaneous velocities, which are driven by white noise. A Gaussian distribution with a tridiagonal correlation matrix accounts for that colored noise and allows a consistent approximation of the likelihood in the limit of small sampling intervals. In contrast to filtering approaches [29], this method yields a compact functional form of the likelihood while having the same $\mathcal{O}(M)$ computational com-

plexity.

Samples drawn proportional to the single trajectory likelihoods can be used in an EM algorithm to obtain a maximum likelihood estimate for the parameters of the heterogeneity distribution. We proposed to use importance sampling in order to avoid resampling at each step of the algorithm. Using the same set of samples, the Hessian matrix of the heterogeneity likelihood can be approximated which provides an uncertainty measure that captures the variability of the estimator under different realizations.

We note, that once the heterogeneity has been inferred, it can also be used to improve the estimate of the individual motility parameters in the spirit of Eq. (30).

The applicability of the inference method presented in this paper relies on a number of assumptions. We discuss them in the following and point at possible generalizations that loosen these assumptions.

First, we have assumed a constant time τ between measurements. In experimental setting individual measurements are sometimes not recorded correctly resulting in missing data points in trajectories. This leads to a time between measurements that is a multiple of τ . Our method can be adapted to these cases: the missing data can be included in the sampling process of the motility parameters and subsequently marginalized, such that the motility parameters are effectively sampled from the likelihood with respect to the available data points. For cases with irregular measurements, there is no timescale τ and therefore a secant velocity cannot be defined consistently across a trajectory. However, it should still be possible to set up an equivalent of Eq. (21) where the right hand side has more complicated statistics which depend on the durations between the measurements. The potential advantages of such an approach compared to extended Kalman filters [29, 38] remain to be evaluated.

Furthermore, we assumed that there is no measurement error and positions can be measured exactly. This

is a valid approximation e. g. for observations of cells with amoeboid motility [52] where the area center of the cell can be calculated with sub-pixel accuracy. In other scenarios, it might be necessary to take the measurement uncertainties into account. In these cases, the measurements become

$$\mathbf{y}_j = \mathbf{x}_j + \boldsymbol{\varepsilon}_j, \quad (39)$$

with $\boldsymbol{\varepsilon}_j$ representing the measurement noise. The measured noisy secant velocities will then take the form

$$\boldsymbol{\nu}_j = \frac{\mathbf{y}_{j+1} - \mathbf{y}_j}{\tau} = \mathbf{V}_j + \frac{\boldsymbol{\nu}_j}{\tau}, \quad (40)$$

where $\boldsymbol{\nu}_j := \boldsymbol{\varepsilon}_{j+1} - \boldsymbol{\varepsilon}_j$. Note, that the noise terms $\boldsymbol{\nu}_j$ in Eq. (40) are correlated with their neighbors. The single trajectory likelihood with respect to the measured secant velocities is given as

$$p(\boldsymbol{\nu}_{0:M-1}|\boldsymbol{\eta}) = \int (d\mathbf{V})^M p(\boldsymbol{\nu}_{0:M-1}|\mathbf{V}_{0:M-1}) p(\mathbf{V}_{0:M-1}|\boldsymbol{\eta}). \quad (41)$$

The integrals above are generally untractable analytically, but could be evaluated numerically. It remains to be studied if measurement uncertainty can be approximately treated in the sequential evaluation of the Gaussian density as presented in Appendix F.

In this paper, we have considered drifts that depend on velocity only. Additional position dependence of the drift can be included in the derivation of the transformed Gaussian method without altering the scaling behavior of the correction term. Note, that in this case an additional term for the steady state distribution of the initial position \mathbf{x}_0 is needed.

Extensions to models with noise multiplicative in the velocity are not readily possible under the current framework, though. In the drift in Eq. (17), the instantaneous velocity could just be replaced by the secant velocity which only introduced a $\mathcal{O}(\tau)$ correction. Doing the same with a multiplicative noise term would lead to correction terms larger than $\mathcal{O}(\tau)$. It remains to be studied if the additional correction terms or more intricate modifications still allow for consistent likelihood approximations in the spirit of the transformed Gaussian method. Alternative methods to tackle models with multiplicative noise are Gaussian filter approaches [29] possibly enhanced by Taylor moment expansions [53] or using full blown particle methods [30, 31].

We see our approach as a step on the way to analyzing the variability and heterogeneity of motility patterns more thoroughly. While we have considered MLEs in this work, the method can readily be used in Bayesian frameworks. Provided with a prior on $\boldsymbol{\theta}$, the EM algorithm can be modified to obtain a maximum posterior estimate [54, chap. 9.4]. Additionally, the transformed Gaussian method can also be used in sampling schemes that draw samples from the posterior distribution. When applied to real data, the method can be augmented by

model comparison techniques in order to find the models that best describe the given system. A further future direction is to include interaction terms in the motility model in order to be able to extract heterogeneity within collective motion patterns [55–57], the response to external fields [58] and particle-wall interactions [59]. Finally, we note that our approach is not restricted to motility data. The method for likelihood calculation can in general be applied to systems in which a smoothed out version of the input data is observed, as for example in ice-core data [60].

ACKNOWLEDGMENTS

This research has been partially funded by the Deutsche Forschungsgemeinschaft (DFG) – Project-ID 318763901 – SFB1294.

Appendix A: Correlations of secant velocities for an Ornstein-Uhlenbeck process

Consider the OU process in velocity given in Eq. (5) and observations of the position $\{x_j\}$ after constant time intervals τ . We are interested in the statistics of the secant velocities

$$\mathbf{V}_j = \frac{1}{\tau} \int_{t_j}^{t_{j+1}} dt \mathbf{v}(t) = \frac{\mathbf{x}_{j+1} - \mathbf{x}_j}{\tau}. \quad (A1)$$

All moments can be calculated analytically using the integral formulation above and exploiting the white noise properties. The means and covariances of the secant velocities are given by

$$\mathbb{E}[\mathbf{V}_j] = 0 \quad (A2a)$$

$$\mathbb{E}[V_j^\alpha V_j^\beta] = \frac{2D}{\gamma^3 \tau^2} (e^{-\gamma\tau} - (1 - \gamma\tau)) \delta_{\alpha\beta} \quad (A2b)$$

$$\mathbb{E}[V_j^\alpha V_k^\beta] = \frac{2D}{\gamma^3 \tau^2} e^{-\gamma|j-k|\tau} (\cosh(\gamma\tau) - 1) \delta_{\alpha\beta}, \quad (A2c)$$

where Greek upper indices indicate components of vectors and the last equation is valid for $j \neq k$. The small τ expansions of the expressions are

$$\mathbb{E}[V_j^\alpha V_j^\beta] = \left(\frac{D}{\gamma} - \frac{D\tau}{3} + \mathcal{O}(\tau^2) \right) \delta_{\alpha\beta}, \quad (A3a)$$

$$\mathbb{E}[V_j^\alpha V_k^\beta] = \left(\frac{D}{\gamma} - |j-k|D\tau + \mathcal{O}(\tau^2) \right) \delta_{\alpha\beta}. \quad (A3b)$$

Appendix B: Autocorrelation functions of diffusion processes

In Section III B, we use the autocorrelation function of a stationary diffusion process. We need its leading behavior around zero, which we derive in this section.

Let us consider a one-dimensional process with non-linear drift and additive noise:

$$\dot{v} = f(v) + \sqrt{2D}\xi. \quad (\text{B1})$$

For $s > t$, the autocorrelation function can be written as

$$\mathbb{E}[v(s)v(t)] = \mathbb{E}[v(t)\mathbb{E}[v(s)|v(t)]]. \quad (\text{B2})$$

If the time difference $\tau := s - t$ is small, the transition probability $p(v(s)|v(t))$ becomes Gaussian with mean $v(t) + f(v(t))\tau$ [61]. This implies that autocorrelation function for small τ is

$$\mathbb{E}[v(t+\tau)v(t)] = \mathbb{E}[v(t)^2] + \mathbb{E}[v(t)f(v(t))]\tau. \quad (\text{B3})$$

For stationary processes the two expectation values on the RHS will be time-independent constants. This means that Eq. (B3) has the form assumed in Section III B.

For processes that are not driven by white noise, the leading order behavior of the autocorrelation function can be different. If the autocorrelation function has the form $\mathbb{E}[v(0)v(t)] = c_0 + c_1 t^{2h}$ for $t \ll 1$ with $h > 0$, the bias factor b between $\mathbb{E}[\Delta v \Delta v]$ and $\mathbb{E}[\Delta V \Delta V]$ which is $2/3$ in Eq. (14) becomes

$$b = \frac{2(4^h - 1)}{(1+h)(1+2h)}. \quad (\text{B4})$$

The same factor is found in Ref. [42], where the considered processes are fractional Brownian motion with Hurst index h .

Appendix C: Smoothing kernels: functions and derivatives

Consider an integral transform of a function $v(t)$ with a smoothing kernel $K(s)$ of the form

$$\mathbf{V}(t) = \int_{-\infty}^{\infty} K(t' - t) \mathbf{v}(t') dt' \quad (\text{C1})$$

$$= \int_{-\infty}^{\infty} K(s) \mathbf{v}(t+s) ds. \quad (\text{C2})$$

We assume that the kernel vanishes at $\pm\infty$ and is normalized such that $\int K(s) ds = 1$. The time derivative of $\mathbf{V}(t)$ is then given as

$$\dot{\mathbf{V}}(t) = \frac{d}{dt} \mathbf{V}(t) = \int_{-\infty}^{\infty} K(s) \frac{d}{dt} \mathbf{v}(t+s) ds \quad (\text{C3})$$

$$= \int_{-\infty}^{\infty} K(s) \dot{\mathbf{v}}(t+s) ds. \quad (\text{C4})$$

This means that the derivative of the transformed function is just the transform of the derivative. For a box kernel $K(s) = \frac{1}{\tau}(\Theta(s) - \Theta(s - \tau)) =: B(s)$, where $\Theta(s)$

is the Heaviside-function, we recover the averaging over an interval τ . This is the focus of the main text.

Let us consider the transformation of a function $h(\mathbf{v}(t))$. Expanding $h(\mathbf{v}(u))$ around $\mathbf{V}(t)$ we obtain

$$h(\mathbf{v}(u)) = h(\mathbf{V}(t)) + \nabla h(\mathbf{V}(t))(\mathbf{v}(u) - \mathbf{V}(t)) + R(u), \quad (\text{C5})$$

where $R(u)$ contains higher powers of $(\mathbf{v}(u) - \mathbf{V}(t))$. Plugging this expansion into the transform, we obtain

$$\int_{-\infty}^{\infty} K(s) h(\mathbf{v}(t+s)) ds = h(\mathbf{V}(t)) + \int_{-\infty}^{\infty} K(s) R(t+s) ds. \quad (\text{C6})$$

Note that the linear term vanishes due to the definition of $\mathbf{V}(t)$. If the kernel only has support on a small interval around zero of size τ and $\mathbf{v}(t)$ is a continuous function, the correction term can be bounded. Let us consider the box-kernel used in the main text. The correction term in Eq. (C6) then becomes $\frac{1}{\tau} \int_t^{t+\tau} R(s) ds$. The leading order term in $R(s)$ will be proportional to $(\mathbf{v}(s) - \mathbf{V}(t))(\mathbf{v}(s) - \mathbf{V}(t))^T$. According to the mean value theorem, for each component α there exists a $\bar{t}_\alpha \in [t, t + \tau]$ such that $v^\alpha(\bar{t}_\alpha) = V^\alpha(t)$. Therefore, $v^\alpha(s) - V^\alpha(t) \sim (t - \bar{t}_\alpha)^{1/2} < \tau^{1/2}$, which means that the whole correction term is $\mathcal{O}(\tau)$. This leads to the correction in Eq. (17).

Appendix D: Statistics of integrated noise terms

The noise term in the SDE for the secant velocity is

$$\zeta(t) = \zeta_t = \frac{1}{\tau} \int_t^{t+\tau} dt' \xi(t'). \quad (\text{D1})$$

As an integral of a Gaussian variable, ζ_t is a Gaussian variable as well. The mean and variance are

$$\mathbb{E}[\zeta_t^\alpha] = \frac{1}{\tau} \int_t^{t+\tau} ds' \mathbb{E}[\xi_{s'}^\alpha] = 0 \quad (\text{D2})$$

$$\mathbb{E}[\zeta_t^\alpha \zeta_{t'}^\beta] = \frac{1}{\tau^2} \int_t^{t+\tau} ds \int_{t'}^{t'+\tau} ds' \mathbb{E}[\xi_s^\alpha \xi_{s'}^\beta] \quad (\text{D3})$$

$$= \frac{1}{\tau} \left(1 - \frac{|\Delta t|}{\tau}\right) \Theta(\tau - |\Delta t|) \delta_{\alpha\beta}, \quad (\text{D4})$$

where $\Delta t := t - t'$, Θ is the Heaviside step function and Greek upper indices indicate components of vectors.

The integration of the SDE for the secant velocity [Eq. (17)] over the measurement intervals leads to noise terms of the form

$$\chi_i = \int_{t_i}^{t_i+\tau} dt \zeta(t), \quad (\text{D5})$$

which are again Gaussian with zero mean. The correlations for different components are zero, too. For the same component they can be calculated as follows. Let us first look at the variance:

$$\mathbb{E}[\chi_i^\alpha \chi_i^\alpha] = \int_{t_i}^{t_i+\tau} ds \int_{t_i}^{t_i+\tau} ds' \mathbb{E}[\zeta_s^\alpha \zeta_{s'}^\alpha] \quad (\text{D6})$$

$$\begin{aligned} &= \int_{t_i}^{t_i+\tau} ds \int_{t_i}^{t_i+\tau} ds' \frac{1}{\tau} \left(1 - \frac{|s-s'|}{\tau}\right) \\ &= \frac{4}{6} \tau. \end{aligned} \quad (\text{D7})$$

Next, we calculate the correlation of noise terms shifted by τ :

$$\mathbb{E}[\chi_i^\alpha \chi_{i+1}^\alpha] = \int_{t_i}^{t_i+\tau} ds \int_{t_i+\tau}^{t_i+2\tau} ds' \mathbb{E}[\zeta_s^\alpha \zeta_{s'}^\alpha] \quad (\text{D8})$$

$$\begin{aligned} &= \int_{t_i}^{t_i+\tau} ds \int_{t_i+\tau}^{s+\tau} ds' \frac{1}{\tau} \left(1 - \frac{|s-s'|}{\tau}\right) \\ &= \frac{\tau}{6}. \end{aligned} \quad (\text{D9})$$

All other correlations $\mathbb{E}[\chi_i^\alpha \chi_j^\alpha]$ with $|i-j| > 1$ vanish because the Heaviside function will be zero over the whole integration area. Therefore, we obtain the tridiagonal correlation matrix [Eq. (19)].

Appendix E: Jacobi determinant for transformations

Let us consider two sets of vectors $\{\mathbf{y}_i\}_{i=1,\dots,S}$ and $\{\mathbf{z}_i\}_{i=1,\dots,S}$ connected through an invertible transformation

$$\mathbf{y}_i = \mathbf{g}_1(\mathbf{z}_i) + \mathbf{g}_2(\mathbf{z}_{i-1}), \quad (\text{E1})$$

where \mathbf{z}_0 is assumed to be some constant.

The absolute Jacobi determinant of the above transformation $|\det \partial \mathbf{y} / \partial \mathbf{z}|$ translates between the probability densities of the two sets, if both sets of vectors are random variables. The corresponding Jacobi matrix has the following block entries:

$$\frac{\partial \mathbf{y}_i}{\partial \mathbf{z}_i} = \mathbf{J}[\mathbf{g}_1(\mathbf{x})]|_{\mathbf{x}=\mathbf{z}_i} \quad (\text{E2})$$

and

$$\frac{\partial \mathbf{y}_i}{\partial \mathbf{z}_{i-1}} = \mathbf{J}[\mathbf{g}_2(\mathbf{x})]|_{\mathbf{x}=\mathbf{z}_{i-1}}, \quad (\text{E3})$$

where $\mathbf{J}[\cdot]$ denotes the Jacobi matrix of the function. All other entries are zero. The triangular block structure means that the determinant factorizes and is calculated

as the product of the block determinants on the diagonal. We obtain

$$|\det \partial \mathbf{y} / \partial \mathbf{z}| = \prod_i |\mathbf{J}[\mathbf{g}_1(\mathbf{x})]|_{\mathbf{x}=\mathbf{z}_i}. \quad (\text{E4})$$

After a simple shift of indices, the above can be applied to the transformation in Eq. (22). While Eq. (22) is not guaranteed to be invertible on its whole domain, it will become invertible on the relevant domain in the limit of small τ .

Appendix F: Sequential Calculation of Gaussian Density of $Q_{0:M-2}$

The transformed Gaussian method to calculate the likelihood [Eq. (25)] includes the evaluation of the multivariate Gaussian density approximation of $Q_{0:M-2}$ [Eq. (23)]. This is just a rescaled version of the density of $\chi_{0:M-2}$:

$$p(\chi_{0:M-2}) \approx e^{-\frac{1}{2} \chi_i [\mathbf{Z}^{-1}]_{ij} \chi_j} \det(2\pi \mathbf{Z})^{-1/2}, \quad (\text{F1})$$

where we used Einstein's summation convention with indices $i, j = 0, \dots, M-2$. Due to indices starting with 0 in the main text, we stick to this convention here. Note, that this means that in the following the highest index in a $j \times j$ matrix will be $j-1$ as in the programming languages C or Python. Even though matrix \mathbf{Z} , which is given in Eq. (19), has an explicit inversion formula [62], a straight forward evaluation of the above probability density still requires $\mathcal{O}(M^2)$ calculations due to the double sum in the exponent. In this section we show that there exists a sequential method for evaluation which only takes $\mathcal{O}(M)$ calculations dramatically decreasing the computational complexity.

We first note that the joint probability of $\chi_{0:M-2}$ can be written as conditioned probabilities in the following way:

$$p(\chi_{0:M-2}) = p(\chi_0) \prod_{j=0}^{M-3} p(\chi_{j+1} | \chi_{0:j}). \quad (\text{F2})$$

Since the joint probability density is Gaussian, the conditioned probabilities are as well:

$$p(\chi_j | \chi_{0:j-1}) =: \mathcal{N}(\mu_j, \sigma_j^2). \quad (\text{F3})$$

These densities can be calculated sequentially as we shall see. We let $\mathbf{Z}_{j \times j}$ denote the $j \times j$ version of \mathbf{Z} . Using the rules for partitioned Gaussians (see Ref. [54, chap. 2]), we find that

$$\begin{aligned} \mu_j &= \mathbb{E}[\chi_j] + [\mathbf{Z}_{j+1 \times j+1}]_{jk} [\mathbf{Z}_{j \times j}^{-1}]_{kl} (\chi_l - \mathbb{E}[\chi_l]) \\ &= [\mathbf{Z}_{j+1 \times j+1}]_{j,j-1} [\mathbf{Z}_{j \times j}^{-1}]_{j-1,l} \chi_l, \end{aligned} \quad (\text{F4})$$

where the Einstein sums run over indices $k, l = 0, \dots, j-1$, and

$$\sigma_j^2 = \left([\mathbf{Z}_{j+1 \times j+1}^{-1}]_{jj} \right)^{-1}. \quad (\text{F5})$$

According to Ref. [62], the elements of the inverse of a $j \times j$ matrix $\mathbf{Z}_{j \times j}$ are

$$[\mathbf{Z}_{j \times j}^{-1}]_{kl} = \frac{6}{\tau} (\omega_{|k-l|} - \omega_{|l+l+2|}) \quad (\text{F6})$$

with

$$\omega_m = \frac{\beta^{m+1} + \beta^{2j-m+3}}{(\beta^2 - 1)(1 - \beta^{2(j+1)})}, \quad (\text{F7})$$

where $\beta = -2 + \sqrt{3}$ and $i, j = 0, \dots, k-1$. With this, we find that the variances are

$$\sigma_j^2 = \frac{\tau}{6} (-\beta)^{-1} \frac{1 - \beta^{2(j+2)}}{1 - \beta^{2(j+1)}}. \quad (\text{F8})$$

The mean of the conditioned probabilities are given by

$$\mu_j = \sum_{l=0}^{j-1} \frac{\beta^{j+l+2} - \beta^{j-l}}{1 - \beta^{2(j+1)}} \chi_l \quad (\text{F9})$$

from which it follows that

$$\mu_{j+1} = \frac{1 - \beta^{2(j+1)}}{1 - \beta^{2(j+2)}} \beta (\mu_j - \chi_j). \quad (\text{F10})$$

Therefore, using Eqs. (F8) and (F10) starting from $\mu_0 = 0$, we can indeed calculate $p(\chi_{0:M-2})$ in $\mathcal{O}(M)$ steps. In order to calculate $p(Q_{0:M-2})$, we only need to replace $\tau/6 \rightarrow 2D\tau/6$ in Eq. (F8).

Appendix G: Rewriting the Hessian matrix of the log-likelihood

We consider the log-likelihood of the heterogeneity parameters $\boldsymbol{\theta}$ with respect to the observed trajectories $\{\mathbf{T}^n\}$

$$\log p(\{\mathbf{T}^n\} | \boldsymbol{\theta}) = \sum_n \log \int p(\mathbf{T}^n | \boldsymbol{\eta}) p_{\boldsymbol{\eta}}(\boldsymbol{\eta} | \boldsymbol{\theta}) d\boldsymbol{\eta}. \quad (\text{G1})$$

The elements of the Hessian matrix \mathbf{H} are given by $[\mathbf{H}]_{\alpha\beta} = H_{\alpha\beta} = \partial_{\alpha} \partial_{\beta} \log p(\{\mathbf{T}^n\} | \boldsymbol{\theta})$, where ∂_{α} denotes a derivative with respect to the α -component of $\boldsymbol{\theta}$. In the following we will manipulate the expression of the elements of the Hessian matrix:

$$\begin{aligned} \partial_{\alpha} \partial_{\beta} \log p(\{\mathbf{T}^n\} | \boldsymbol{\theta}) &= \sum_n \partial_{\alpha} \frac{\partial_{\beta} p(\mathbf{T}^n | \boldsymbol{\theta})}{p(\mathbf{T}^n | \boldsymbol{\theta})} \\ &= \sum_n \left[\frac{\partial_{\alpha} \partial_{\beta} p(\mathbf{T}^n | \boldsymbol{\theta})}{p(\mathbf{T}^n | \boldsymbol{\theta})} - \frac{\partial_{\alpha} p(\mathbf{T}^n | \boldsymbol{\theta})}{p(\mathbf{T}^n | \boldsymbol{\theta})} \frac{\partial_{\beta} p(\mathbf{T}^n | \boldsymbol{\theta})}{p(\mathbf{T}^n | \boldsymbol{\theta})} \right] \\ &= \sum_n \left[\frac{\int p(\mathbf{T}^n | \boldsymbol{\eta}) \partial_{\alpha} \partial_{\beta} p_{\boldsymbol{\eta}}(\boldsymbol{\eta} | \boldsymbol{\theta}) d\boldsymbol{\eta}}{p(\mathbf{T}^n | \boldsymbol{\theta})} \right. \\ &\quad \left. - \frac{\int p(\mathbf{T}^n | \boldsymbol{\eta}) \partial_{\alpha} p_{\boldsymbol{\eta}}(\boldsymbol{\eta} | \boldsymbol{\theta}) d\boldsymbol{\eta}}{p(\mathbf{T}^n | \boldsymbol{\theta})} \right. \\ &\quad \left. \times \frac{\int p(\mathbf{T}^n | \boldsymbol{\eta}) \partial_{\beta} p_{\boldsymbol{\eta}}(\boldsymbol{\eta} | \boldsymbol{\theta}) d\boldsymbol{\eta}}{p(\mathbf{T}^n | \boldsymbol{\theta})} \right]. \quad (\text{G2}) \end{aligned}$$

By multiplying each of the integrands in Eq. (G2) by $1 = p_{\boldsymbol{\eta}}(\boldsymbol{\eta} | \boldsymbol{\theta}) / p_{\boldsymbol{\eta}}(\boldsymbol{\eta} | \boldsymbol{\theta})$ and noting that $p(\boldsymbol{\eta} | \mathbf{T}^n, \boldsymbol{\theta}) = p(\boldsymbol{\eta}, \mathbf{T}^n | \boldsymbol{\theta}) / p(\mathbf{T}^n | \boldsymbol{\theta})$, we obtain

$$\begin{aligned} H_{\alpha\beta} &= \sum_n \left[\mathbb{E}_n \left[\frac{\partial_{\alpha} \partial_{\beta} p_{\boldsymbol{\eta}}(\boldsymbol{\eta} | \boldsymbol{\theta})}{p_{\boldsymbol{\eta}}(\boldsymbol{\eta} | \boldsymbol{\theta})} \right] \right. \\ &\quad \left. - \mathbb{E}_n \left[\frac{\partial_{\alpha} p_{\boldsymbol{\eta}}(\boldsymbol{\eta} | \boldsymbol{\theta})}{p_{\boldsymbol{\eta}}(\boldsymbol{\eta} | \boldsymbol{\theta})} \right] \mathbb{E}_n \left[\frac{\partial_{\beta} p_{\boldsymbol{\eta}}(\boldsymbol{\eta} | \boldsymbol{\theta})}{p_{\boldsymbol{\eta}}(\boldsymbol{\eta} | \boldsymbol{\theta})} \right] \right] \Big|_{\boldsymbol{\theta}=\hat{\boldsymbol{\theta}}}, \quad (\text{G3}) \end{aligned}$$

where $\mathbb{E}_n[\cdot]$ denotes expectation values with respect to $p(\boldsymbol{\eta} | \mathbf{T}^n, \boldsymbol{\theta})$. The above is the expression used in the main text. In Ref. [29], Louis' formula from Ref. [51] was applied, which has the form

$$\begin{aligned} H_{\alpha\beta} &= \mathbb{E}[\partial_{\alpha} \partial_{\beta} \log p(\{\mathbf{T}^n\}, \{\boldsymbol{\eta}^n\} | \boldsymbol{\theta})] \\ &\quad + \text{Cov}[\partial_{\gamma} \log p(\{\mathbf{T}^n\}, \{\boldsymbol{\eta}^n\} | \boldsymbol{\theta})], \quad (\text{G4}) \end{aligned}$$

where the expectations are taken with respect to $p(\{\boldsymbol{\eta}^n\} | \{\mathbf{T}^n\}, \boldsymbol{\theta})$. This is equivalent to Eq. (G3).

-
- [1] T. Vicsek and A. Zafeiris, Collective motion, *Phys. Rep.* **517**, 71 (2012).
 - [2] P. Romanczuk, M. Bär, W. Ebeling, B. Lindner, and L. Schimansky-Geier, Active Brownian particles: From individual to collective stochastic dynamics, *Eur. Phys. J.: Spec. Top.* **202**, 1 (2012).
 - [3] M. C. Marchetti, J. F. Joanny, S. Ramaswamy, T. B. Liverpool, J. Prost, M. Rao, and R. A. Simha, Hydrodynamics of soft active matter, *Rev. Mod. Phys.* **85**, 1143 (2013).
 - [4] E. Méhes and T. Vicsek, Collective motion of cells: from experiments to models, *Integr. Biol.* **6**, 831 (2014).
 - [5] C. Bechinger, R. Di Leonardo, H. Löwen, C. Reichardt, G. Volpe, and G. Volpe, Active particles in complex and crowded environments, *Rev. Mod. Phys.* **88**, 045006 (2016).

- [6] A. Cavagna, L. Del Castello, I. Giardina, T. Grigera, A. Jelic, S. Melillo, T. Mora, L. Parisi, E. Silvestri, M. Viale, and A. M. Walczak, Flocking and turning: A new model for self-organized collective motion, *J. Stat. Phys.* **158**, 601 (2015).
- [7] J. Gautrais, F. Ginelli, R. Fournier, S. Blanco, M. Soria, H. Chaté, and G. Theraulaz, Deciphering interactions in moving animal groups, *PLOS Comput. Biol.* **8**, e1002678 (2012).
- [8] G. Ariel and A. Ayali, Locust collective motion and its modeling, *PLOS Comput. Biol.* **11**, e1004522 (2015).
- [9] A. Corbetta, C.-m. Lee, R. Benzi, A. Muntean, and F. Toschi, Fluctuations around mean walking behaviors in diluted pedestrian flows, *Phys. Rev. E* **95**, 032316 (2016).

- (2017).
- [10] D. Selmecki, L. Li, L. I. Pedersen, S. F. Nrrlykke, P. H. Hagedorn, S. Mosler, N. B. Larsen, E. C. Cox, and H. Flyvbjerg, Cell motility as random motion: A review, *Eur. Phys. J.: Spec. Top.* **157**, 1 (2008).
 - [11] G. Anselem, M. Theves, A. Bae, E. Bodenschatz, and C. Beta, A stochastic description of *dictyostelium* chemotaxis, *PLOS ONE* **7**, e37213 (2012).
 - [12] J. N. Pedersen, L. Li, C. Grădinaru, R. H. Austin, E. C. Cox, and H. Flyvbjerg, How to connect time-lapse recorded trajectories of motile microorganisms with dynamical models in continuous time, *Phys. Rev. E* **94**, 062401 (2016).
 - [13] A. Klimek, D. Mondal, S. Block, P. Sharma, and R. R. Netz, Data-driven classification of individual cells by their non-Markovian motion, *Biophys. J.* **123**, 1173 (2024).
 - [14] D. B. Brückner and C. P. Broedersz, Learning dynamical models of single and collective cell migration: A review, *Rep. Prog. Phys.* **87**, 056601 (2024).
 - [15] C. E. Meacham and S. J. Morrison, Tumour heterogeneity and cancer cell plasticity, *Nature* **501**, 328 (2013).
 - [16] S. Peled, S. D. Ryan, S. Heidenreich, M. Bär, G. Ariel, and A. Be'er, Heterogeneous bacterial swarms with mixed lengths, *Phys. Rev. E* **103**, 032413 (2021).
 - [17] S. Persson, N. Welkenhuysen, S. Shashkova, S. Wiqvist, P. Reith, G. W. Schmidt, U. Picchini, and M. Cvijovic, Scalable and flexible inference framework for stochastic dynamic single-cell models, *PLOS Comput. Biol.* **18**, e1010082 (2022).
 - [18] G. Ariel, A. Ayali, A. Be'er, and D. Knebel, Variability and heterogeneity in natural swarms: Experiments and modeling, in *Active Particles, Volume 3: Advances in Theory, Models, and Applications*, edited by N. Bellomo, J. A. Carrillo, and E. Tadmor (Springer International Publishing, 2022) pp. 1–33.
 - [19] J. L. Spudich and D. E. Koshland, Non-genetic individuality: Chance in the single cell, *Nature* **262**, 467 (1976).
 - [20] A. J. Waite, N. W. Frankel, Y. S. Dufour, J. F. Johnston, J. Long, and T. Emonet, Non-genetic diversity modulates population performance, *Mol. Syst. Biol.* **12**, 895 (2016).
 - [21] E. Lemaître, I. M. Sokolov, R. Metzler, and A. V. Chechkin, Non-Gaussian displacement distributions in models of heterogeneous active particle dynamics, *New J. Phys.* **25**, 013010 (2023).
 - [22] R. Großmann, L. S. Bort, T. Moldenhawer, M. Stange, S. S. Panah, R. Metzler, and C. Beta, Non-Gaussian displacements in active transport on a carpet of motile cells, *Phys. Rev. Lett.* **132**, 088301 (2024).
 - [23] D. B. Brückner, A. Fink, J. O. Rädler, and C. P. Broedersz, Disentangling the behavioural variability of confined cell migration, *J. R. Soc. Interface* **17**, 20190689 (2020).
 - [24] J. Hasenauer, S. Waldherr, N. Radde, M. Doszczak, P. Scheurich, and F. Allgöwer, A maximum likelihood estimator for parameter distributions in heterogeneous cell populations, *Procedia Comput. Sci.* **1**, 1655 (2010).
 - [25] J. Hasenauer, S. Waldherr, M. Doszczak, P. Scheurich, N. Radde, and F. Allgöwer, Analysis of heterogeneous cell populations: A density-based modeling and identification framework, *J. Process Control* **21**, 1417 (2011).
 - [26] A. Klimek, J. C. J. Heyn, D. Mondal, S. Schwartz, J. O. Rädler, P. Sharma, S. Block, and R. R. Netz, Intrinsic cell-to-cell variance from experimental single-cell motility data, [arXiv:2410.14561](https://arxiv.org/abs/2410.14561) (2024).
 - [27] S. Donnet and A. Samson, A review on estimation of stochastic differential equations for pharmacokinetic/pharmacodynamic models, *Adv. Drug Deliv. Rev.* **65**, 929 (2013).
 - [28] U. Picchini, A. de Gaetano, and S. Ditlevsen, Stochastic differential mixed-effects models, *Scand. J. Stat.* **37**, 67 (2010).
 - [29] M. Delattre and M. Lavielle, Coupling the SAEM algorithm and the extended Kalman filter for maximum likelihood estimation in mixed-effects diffusion models, *Stat. Its Interface* **6**, 519 (2013).
 - [30] G. A. Whitaker, A. Golightly, R. J. Boys, and C. Sherlock, Bayesian inference for diffusion-driven mixed-effects models, *Bayesian Anal.* **12**, 435 (2017).
 - [31] S. Wiqvist, A. Golightly, A. T. McLean, and U. Picchini, Efficient inference for stochastic differential equation mixed-effects models using correlated particle pseudo-marginal algorithms, *Comput. Stat. Data Anal.* **157**, 107151 (2021).
 - [32] U. Picchini, Stochastic differential equations mixed-effects models, <https://umbertopicchini.github.io/sdemem/>.
 - [33] M. Delattre, A review on asymptotic inference in stochastic differential equations with mixed effects, *Jpn. J. Stat. Data. Sci.* **4**, 543 (2021).
 - [34] H. U. Bödeker, C. Beta, T. D. Frank, and E. Bodenschatz, Quantitative analysis of random ameboid motion, *Europhys. Lett.* **90**, 28005 (2010).
 - [35] D. B. Brückner, P. Ronceray, and C. P. Broedersz, Inferring the dynamics of underdamped stochastic systems, *Phys. Rev. Lett.* **125**, 058103 (2020).
 - [36] F. Ferretti, V. Chardès, T. Mora, A. M. Walczak, and I. Giardina, Building general Langevin models from discrete datasets, *Phys. Rev. X* **10**, 031018 (2020).
 - [37] C. Metzner, C. Mark, J. Steinwachs, L. Lautscham, F. Stadler, and B. Fabry, Superstatistical analysis and modelling of heterogeneous random walks, *Nat. Commun.* **6**, 7516 (2015).
 - [38] S. Särkkä, *Bayesian Filtering and Smoothing*, Institute of Mathematical Statistics Textbooks (Cambridge University Press, Cambridge, 2013).
 - [39] M. Delattre, V. Genon-Catalot, and A. Samson, Estimation of population parameters in stochastic differential equations with random effects in the diffusion coefficient, *ESAIM PS* **19**, 671 (2015).
 - [40] V. Genon-Catalot and C. Larédo, Estimation for stochastic differential equations with mixed effects, *Statistics* **50**, 1014 (2016).
 - [41] S. M. Iacus, *Simulation and Inference for Stochastic Differential Equations: With R Examples*, Springer Series in Statistics (Springer, New York, NY, 2008).
 - [42] I. Cialenco, H.-J. Kim, and G. Pasemann, Statistical analysis of discretely sampled semilinear SPDEs: A power variation approach, *Stoch. PDE: Anal. Comp.* **12**, 326 (2024).
 - [43] A. Gloter, Parameter estimation for a discretely observed integrated diffusion process, *Scand. J. Stat.* **33**, 83 (2006).
 - [44] F. Ferretti, V. Chardès, T. Mora, A. M. Walczak, and I. Giardina, Renormalization group approach to connect discrete- and continuous-time descriptions of Gaussian processes, *Phys. Rev. E* **105**, 044133 (2022).
 - [45] J. Albrecht and S. Reich, Robust parameter estimation for partially observed second-order diffusion processes, [arXiv:2406.14738](https://arxiv.org/abs/2406.14738) (2024).

- [46] C. E. Rasmussen and C. K. I. Williams, *Gaussian Processes for Machine Learning* (The MIT Press, 2005).
- [47] B. Liebchen and D. Levis, Chiral active matter, *Europhys. Lett.* **139**, 67001 (2022).
- [48] A. P. Dempster, N. M. Laird, and D. B. Rubin, Maximum likelihood from incomplete data via the EM algorithm, *J. Roy. Statist. Soc. Ser. B* **39**, 1 (1977).
- [49] C. Robert and R. Casella, *Monte Carlo Statistical Methods*, 2nd ed., Springer Texts in Statistics (Springer New York, 2004).
- [50] M. J. Schervish, *Theory of Statistics*, Springer Series in Statistics (Springer New York, 1995).
- [51] T. A. Louis, Finding the observed information matrix when using the EM algorithm, *J. Roy. Statist. Soc. Ser. B* **44**, 226 (1982).
- [52] A. G. Cherstvy, O. Nagel, C. Beta, and R. Metzler, Non-Gaussianity, population heterogeneity, and transient superdiffusion in the spreading dynamics of amoeboid cells, *Phys. Chem. Chem. Phys.* **20**, 23034 (2018).
- [53] Z. Zhao, T. Karvonen, R. Hostettler, and S. Särkkä, Taylor moment expansion for continuous-discrete Gaussian filtering, *IEEE Trans. Autom. Control* **66**, 4460 (2021).
- [54] C. Bishop, *Pattern Recognition and Machine Learning* (Springer New York, 2006).
- [55] G. Ariel, O. Rimer, and E. Ben-Jacob, Order-disorder phase transition in heterogeneous populations of self-propelled particles, *J. Stat. Phys.* **158**, 579 (2015).
- [56] P. de Castro, F. M. Rocha, S. Diles, R. Soto, and P. Sollich, Diversity of self-propulsion speeds reduces motility-induced clustering in confined active matter, *Soft Matter* **17**, 9926 (2021).
- [57] R. Supekar, B. Song, A. Hastewell, G. P. T. Choi, A. Mietke, and J. Dunkel, Learning hydrodynamic equations for active matter from particle simulations and experiments, *Proc. Natl. Acad. Sci.* **120**, e2206994120 (2023).
- [58] J. Rode, M. Novak, and B. M. Friedrich, Information theory of chemotactic agents using both spatial and temporal gradient sensing, *PRX Life* **2**, 023012 (2024).
- [59] S. Lambert, M. Duchene, and S. Klumpp, Bayesian inference of wall torques for active Brownian particles, [arXiv:2409.03533](https://arxiv.org/abs/2409.03533) (2024).
- [60] P. D. Ditlevsen, S. Ditlevsen, and K. K. Andersen, The fast climate fluctuations during the stadial and interstadial climate states, *Ann. Glaciol.* **35**, 457 (2002).
- [61] H. Risken, *The Fokker-Planck Equation. Methods of Solutions and Applications.*, 2nd ed., Springer Ser. Synergetics (Berlin: Springer-Verlag, 1996).
- [62] J. Jia, T. Sogabe, and M. El-Mikkawy, Inversion of k-tridiagonal matrices with Toeplitz structure, *Comput. Math. Appl.* **65**, 116 (2013).